Offshore Wind Potential in South India from Synthetic Aperture Radar

Hasager, Charlotte Bay; Bingöl, Ferhat; Badger, Merete; Karagali, Ioanna; Sreevalsan, E.

Publication date:
2011

Document Version
Publisher's PDF, also known as Version of record

Offshore Wind Potential in South India from Synthetic Aperture Radar

Risø-R-Report

Charlotte B. Hasager, Ferhat Bingöl, Merete Badger, Ioanna Karagali, E. Sreevalsan

Risø-R-1780(EN)

October 2011

Risø DTU
National Laboratory for Sustainable Energy

Authors: Charlotte B. Hasager, Ferhat Bingöl, Merete Badger, Ioanna Karagali, E. Sreevalsan
Title: Offshore Wind Potential in South India from Synthetic Aperture Radar
Division: Wind Energy Division

Risø-R-1780(EN)
October 2011

Abstract:
The offshore wind energy potential for pre-feasibility in South India in the area from 77° to 80° Eastern longitude and 7° to 10° Northern latitude is observed from a total of 164 ENVISAT Advanced Synthetic Aperture Radar (ASAR) satellite images during the years 2002 to 2011. All satellite scenes are from Wide Swath Mode and each cover approximately 400 km by 400 km. The ocean wind speed maps are retrieved and processed at Risø DTU. The results show wind energy density from 200 W/m^2 to 500 W/m^2 at 10 m height above sea level. QuikSCAT ocean winds are included as background information on the 10-year mean and a general description of the winds and climate with monsoons in India is presented.

ISSN 0106-2840
ISBN 978-87-550-3908-7

Contract no.:

Group's own reg. no.:
1130610-10

Sponsorship:
Centre for Wind Energy Technology (C-WET), India

Cover :

Pages:
Tables:
References:

Information Service Department
Risø National Laboratory for Sustainable Energy
Technical University of Denmark
P.O.Box 49
DK-4000 Roskilde
Denmark
Telephone +45 46774005
bibl@risoe.dtu.dk
Fax +45 46774013
www.risoe.dtu.dk

Contents

Preface

The project is on mapping offshore winds in South India using Synthetic Aperture Radar (SAR) and scatterometer satellite data. A total of 164 archived scenes from the Advanced SAR instrument on-board the European ENVISAT satellite have been retrieved for the period 2002-2011. In addition, 10 years (1999-2009) of QuikSCAT data from the SeaWinds satellite have been downloaded. Satellite data from the European Space Agency (project C1P.8328) and Remote Sensing Systems is acknowledged.

1 Background

At the Centre for Wind Energy Technology (C-WET) in Chennai, India, there is a need for mapping the offshore winds near the coast in South India. Collaboration between C-WET and Risø DTU is established. Risø DTU has contributed in capacity of satellite based offshore wind resource mapping. This is useful for the initial planning of offshore wind farms. The area of interest is from 77° to 80° Eastern longitude and from 7° to 10° Northern latitude.

2 Methodology

The conventional method used to produce estimates of wind resources is to analyse detailed wind measurements made at one or more sites for at least one year. This criterion is difficult to satisfy offshore where measurements are costly and sparse. Therefore other methods are required – methods that will not meet bankable accuracy in resource estimates, but on the other hand typically give good indications of the geographical distribution of the wind resource and that will be very useful for decision making and planning of feasibility studies and of actual project preparation (if feasible).

Satellite synthetic aperture radar (SAR) data are observations of the small-scale roughness at the sea surface. A number of overlapping SAR images were retrieved over the area of interest in India. Each image was calibrated to show radar backscatter and an inversion scheme was applied to retrieve the wind speed at 10 m.

A software package developed by the Johns Hopkins University, Applied Physics Laboratory in the US was used for the wind retrieval. Retrieval of the 10-m wind speed requires information about the wind direction. Wind directions were obtained from the US Navy Operational Global Atmospheric Prediction System (NOGAPS) at a 1 degree latitude and longitude resolution. These 6-hourly model wind directions were interpolated in time and space to match the SAR data. For 15 of the investigated SAR scenes NOGAPS failed to provide any data around the time of the satellite pass. The wind retrieval software was then run with a constant wind direction obtained from the National Center for Environmental Prediction and the National Center for Atmospheric Research (NCEP/NCAR, USA) reanalysis data set at the location 78.75° E, 8.57° N. The time difference was 1-1.5 hours between the reanalysis data and satellite passes. The wind directions obtained from NCEP/NCAR are listed in Table 1.

The satellite wind fields were combined for wind resource mapping using the Risø DTU tool S-WAsP. The end product is a multi-layer digital map of the offshore wind resource showing the 10-m mean wind speed, energy density, Weibull scale (A) and shape (k) parameters at a 1-km spatial resolution. More detailed statistics such as wind roses and a WAsP .tab file is produced for selected point locations. Further detail on the method please see [1].

Table 1. List of SAR scenes processed using wind directions from the NCEP/NCAR reanalysis data set. Wind directions from NCEP/NCAR are given using the oceanographic convention (i.e. 'blowing towards').

SAR data		NCEP/NCAR data	
YYYYMMDD	HHMMSS	HH	Wind direction
20030103	043443	06	223
20030107	164758	18	238
20030119	043153	06	237
20031111	042909	06	241
20031121	165345	18	224
20031130	043202	06	223
20040507	043448	06	51
20040510	044029	06	112
20040511	164805	18	96
20040523	043203	06	98
20040526	043743	06	81
20051024	165929	18	110
20051217	170212	18	152
20061119	043200	06	224
20081206	170156	18	187

3 SAR winds

We rely on ENVISAT ASAR WSM images from the European Space Agency (ESA). The WSM – Wide Swath Mode – scenes each cover 400 km x 400 km. As examples two of the wind maps are shown in Figure 1 and Figure 2. Figure 1 shows an example from 4 December 2010 characterized by strong winds whereas the Figure 2 shows much weaker winds on 25 September 2010. A total of 164 WSM scenes are used. Most of the 164 scenes are from ESA's ordering system EOLISA and sent on DVD to Risø DTU but a few are taken from ESA's rolling archive.

The number of scenes per year and per month is listed in Table 2. There are a total of 164 ocean wind maps out of which 72 are observed in the morning and 92 in the evening. The distribution through years, months, seasons and early morning vs. early evening is shown in Figure 3. Appendix 1 lists all scenes.

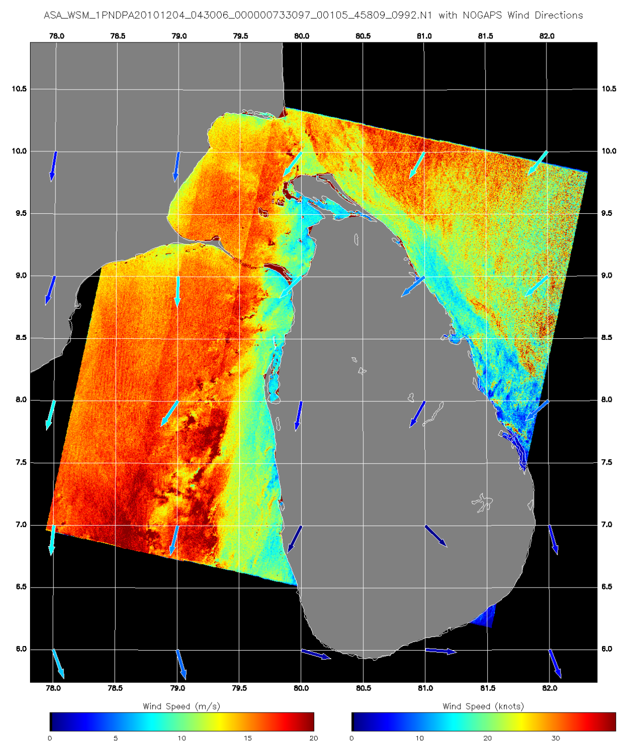

Figure 1.Ocean wind map from ENVISAT ASAR WSM from 4 December 2010 at 04.30 UTC in South India.

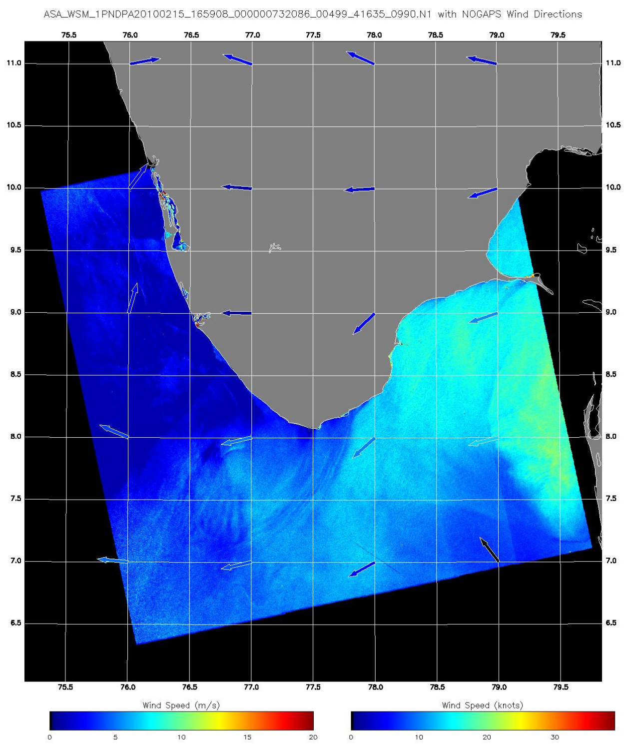

Figure 2.Ocean wind map from ENVISAT ASAR WSM from 25 September 2010 at 04.43 UTC in South India.

Table 2. List of ENVISAT ASAR WSM scenes per year and per month.

Year										
2002	2003	2004	2005	2006	2007	2008	2009	2010	2011	Total
6	31	37	22	21	9	13	16	6	3	164

Month												
1	2	3	4	5	6	7	8	9	10	11	12	Total
10	13	19	14	20	9	8	8	11	15	15	22	164

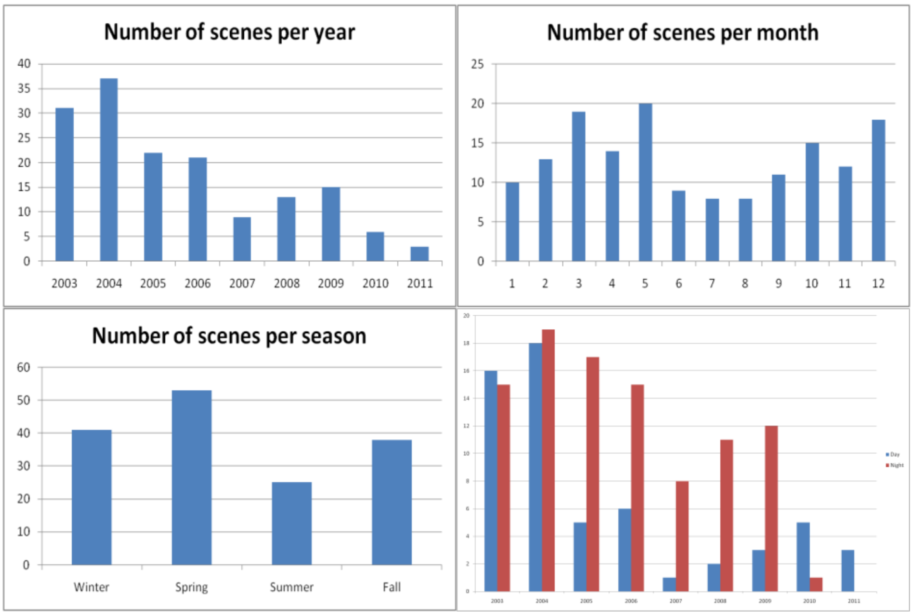

Figure 3.Number of ocean wind maps from ENVISAT ASAR WSM per year (upper left), per month (upper right), per season (lower left) and morning vs. night passes (lower left).

The satellite scenes used for the South India offshore area cover as shown in Figure 4. In the area of interest the number of overlapping scenes varies from 100 to 160 scenes. The calculated offshore mean wind speed is shown in Figure 5. It can be seen that the near-coastal winds are around 4 m/s to 5 m/s while winds further offshore are higher, up to 7.6 m/s. All results reported are for 10 m above sea level.

The Weibull statistics scale (A) and shape (k) parameters are calculated. The results are shown in Figure 6 and Figure 7, respectively. Weibull A varies smoothly from around 6 m/s near the coast to more than 8 m/s further offshore. In contrast, the Weibull k has a patchy appearance related to the track of scenes. This is agreement with the fact that too few samples are available for a reliable estimate of Weibull k, see [2].

Figure 8 shows the wind power density (or wind energy density) calculated based on the 164 ENVISAT ASAR wind maps. The near-coastal zone is around 200 W/m^2 while much higher values are found far offshore, up to more than 500 W/m^2.

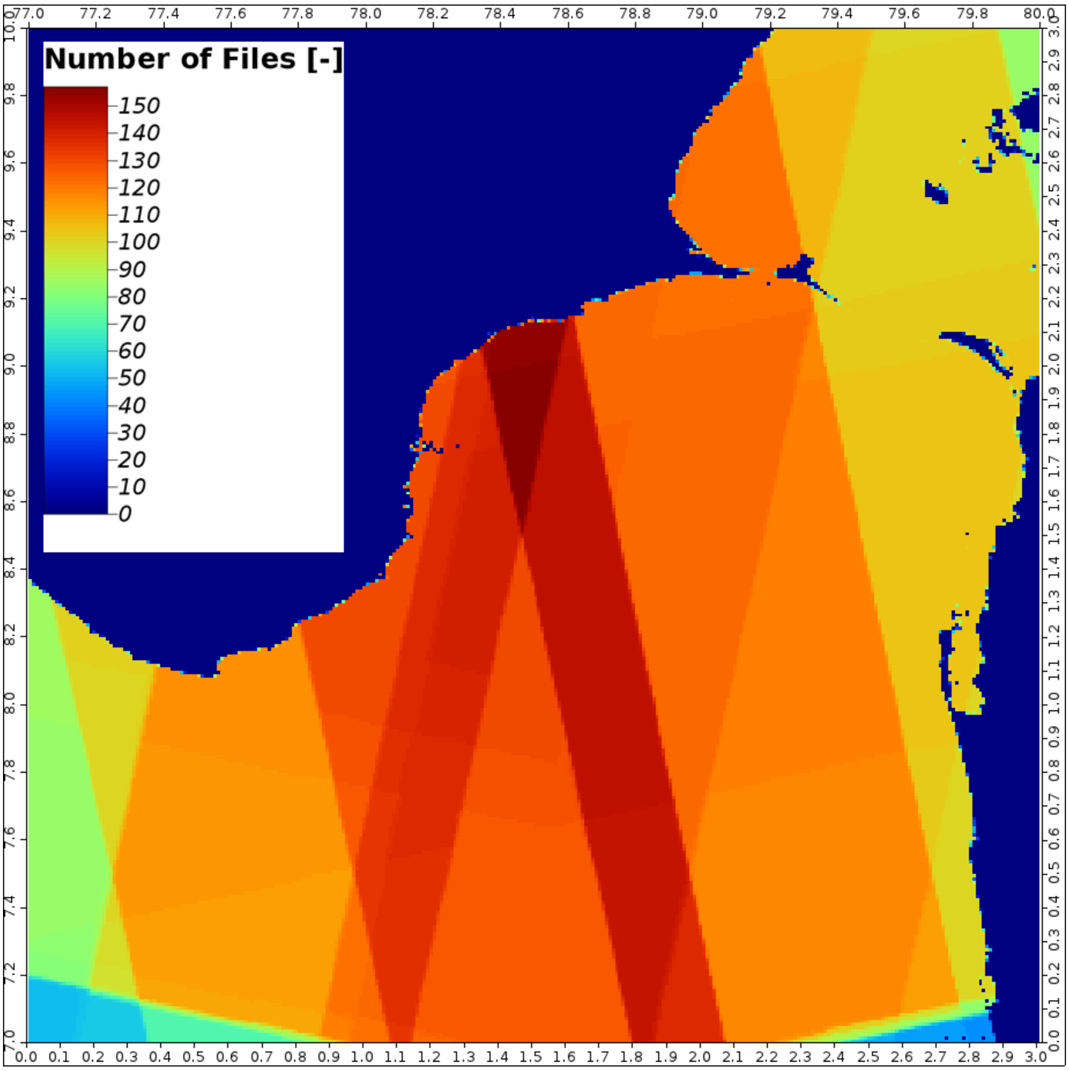

Figure 4.Number of overlapping ENVISAT ASAR wind maps offshore in South India. The coordinates are from 7° to 10° northern latitude and 77° to 80° eastern longitude.

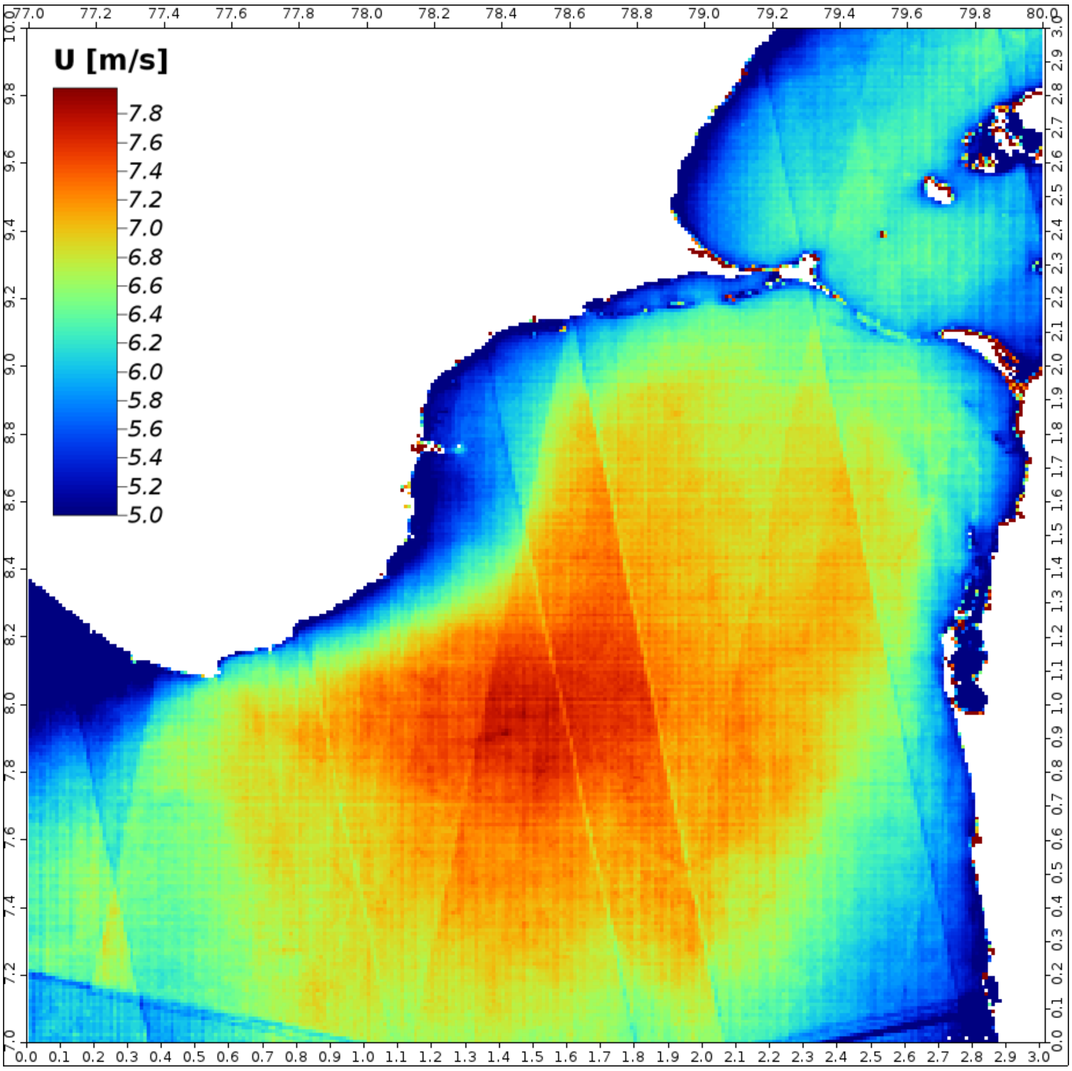

Figure 5.Mean wind speed from 164 ENVISAT ASAR wind maps offshore in South India. The coordinates are from 7° to 10° northern latitude and 77° to 80° eastern longitude.

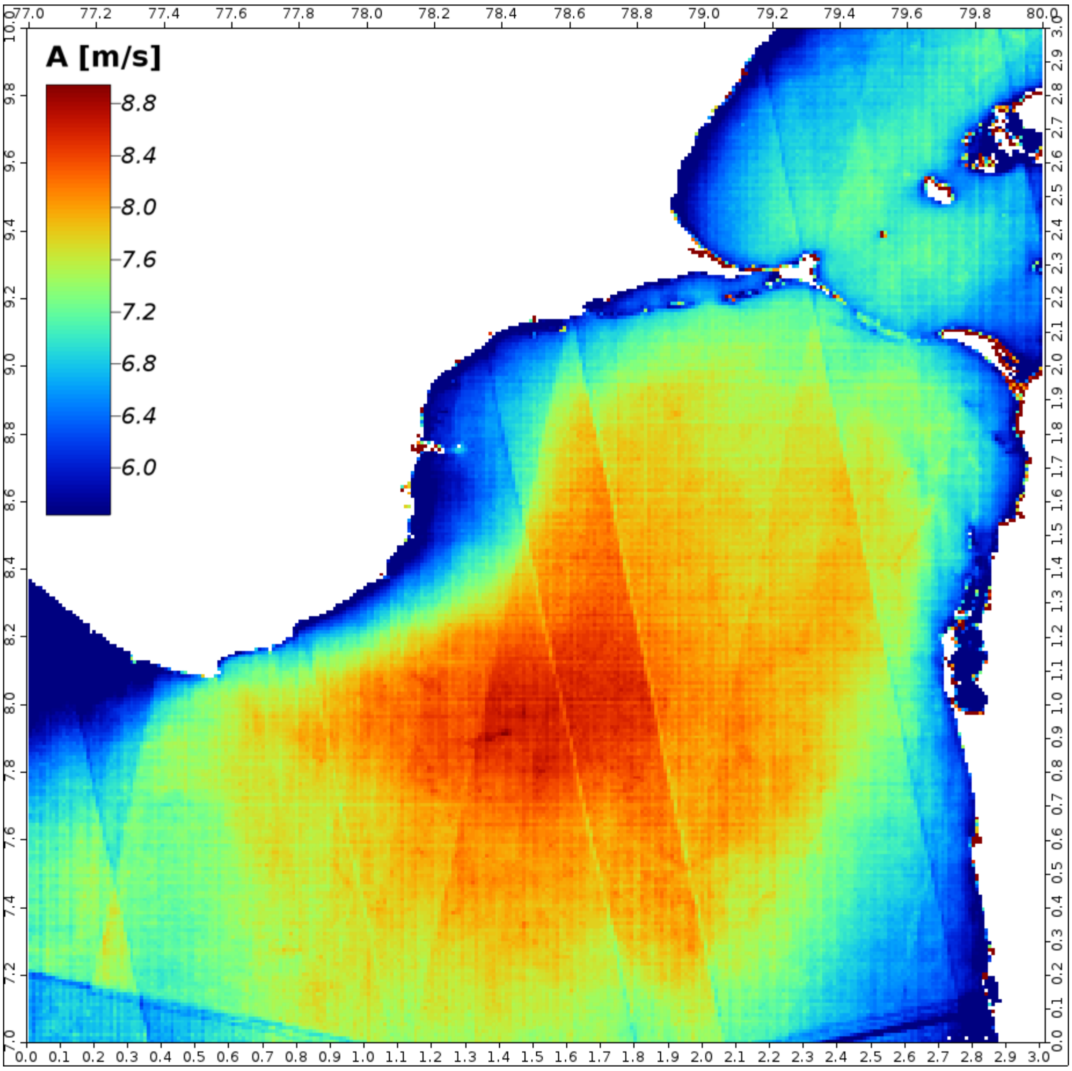

Figure 6. Weibull A observed from 164 ENVISAT ASAR wind maps offshore in South India. The coordinates are from 7° to 10° northern latitude and 77° to 80° eastern longitude.

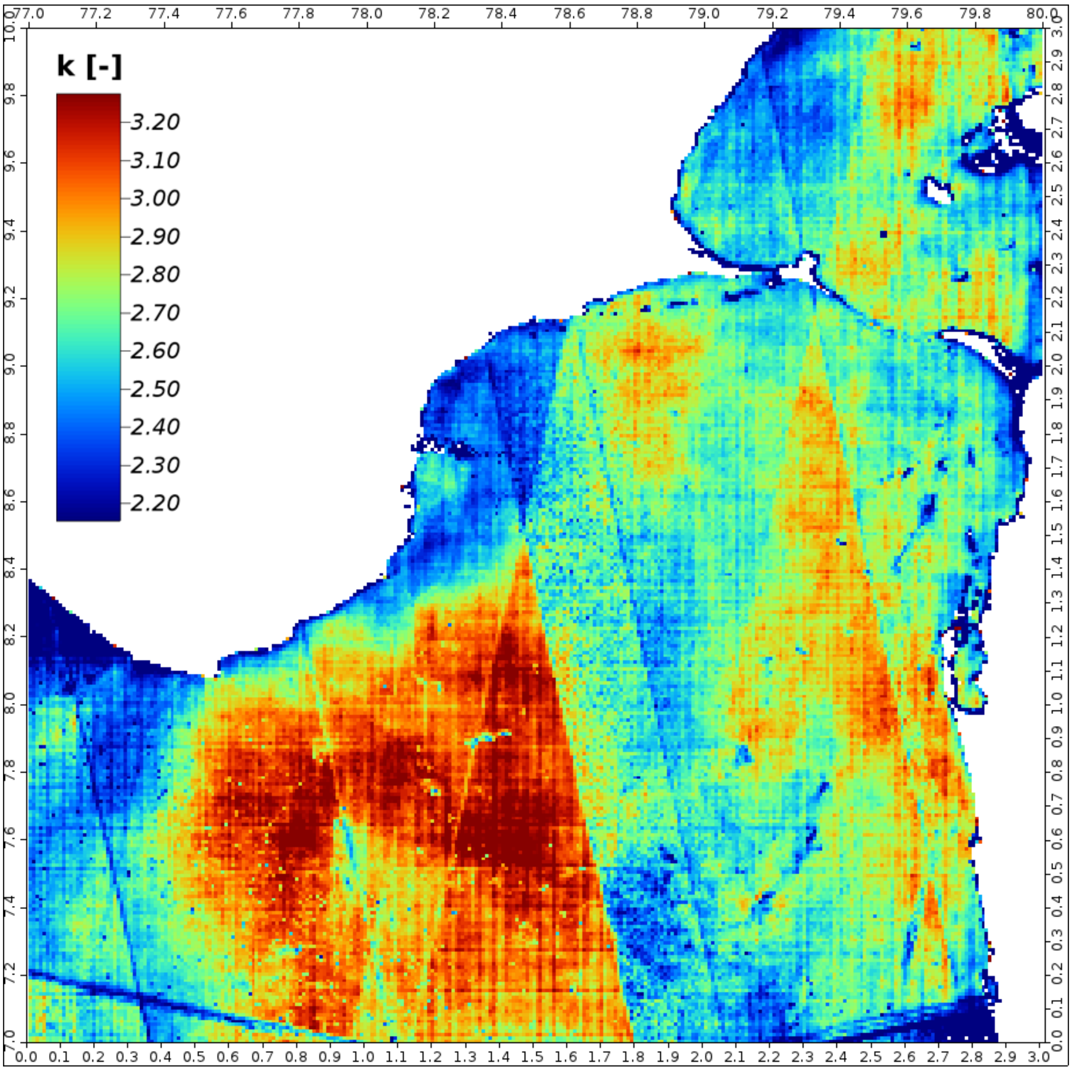

Figure 7. Weibull k observed from 164 ENVISAT ASAR wind maps offshore in South India. The coordinates are from 7° to 10° northern latitude and 77° to 80° eastern longitude.

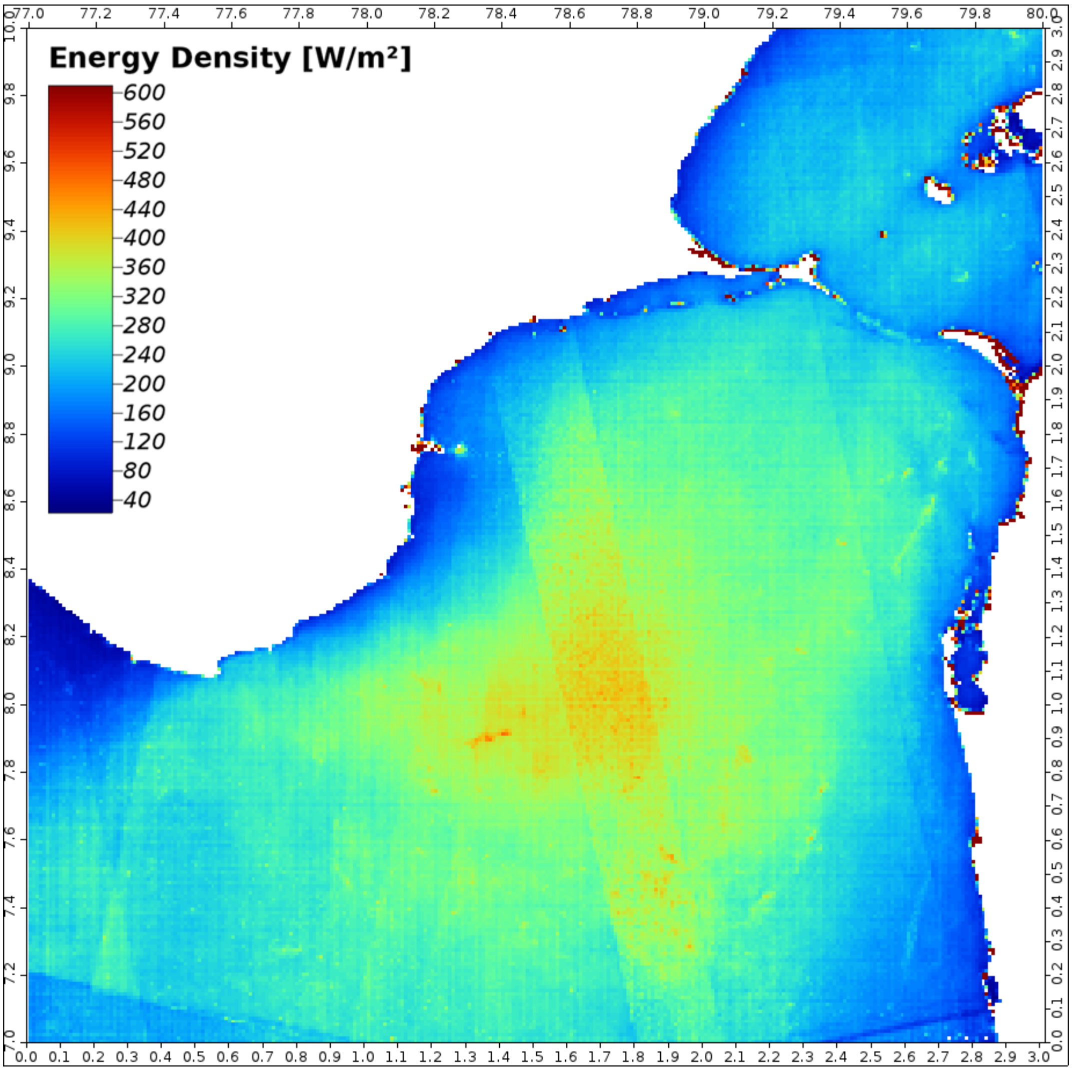

Figure 8. Wind power density observed from 164 ENVISAT ASAR wind maps offshore in South India. The coordinates are from 7° to 10° northern latitude and 77° to 80° eastern longitude.

The mean wind speed and energy density are presented in form of histograms in Figure 9 and Figure 10, respectively. It is seen in Figure 9 that the winds have two peaks, one around 6.1 m/s and another around 6.8 m/s. This may be related to the winds of different seasons (monsoon). Similarly the wind energy density has two peaks, major peak around 260 W/m^2 and minor peak around 300 W/m^2. Generally, the winter monsoon shows winds from the northeast and the summer monsoon from the southeast.

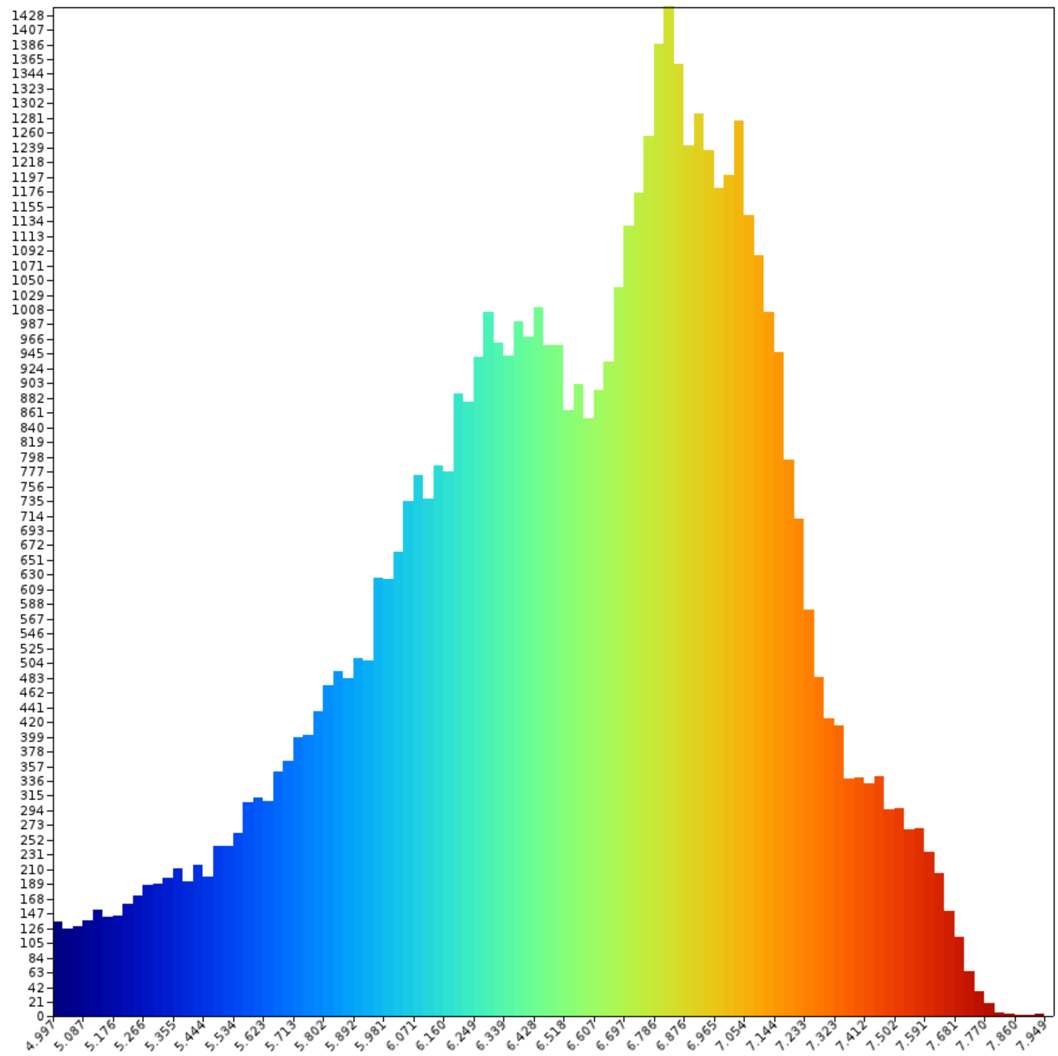

Figure 9. Histogram of wind speed from 164 ENVISAT ASAR wind maps offshore in South India. The x-axis shows wind speed in m/s and y-axis shows number of grid cells.

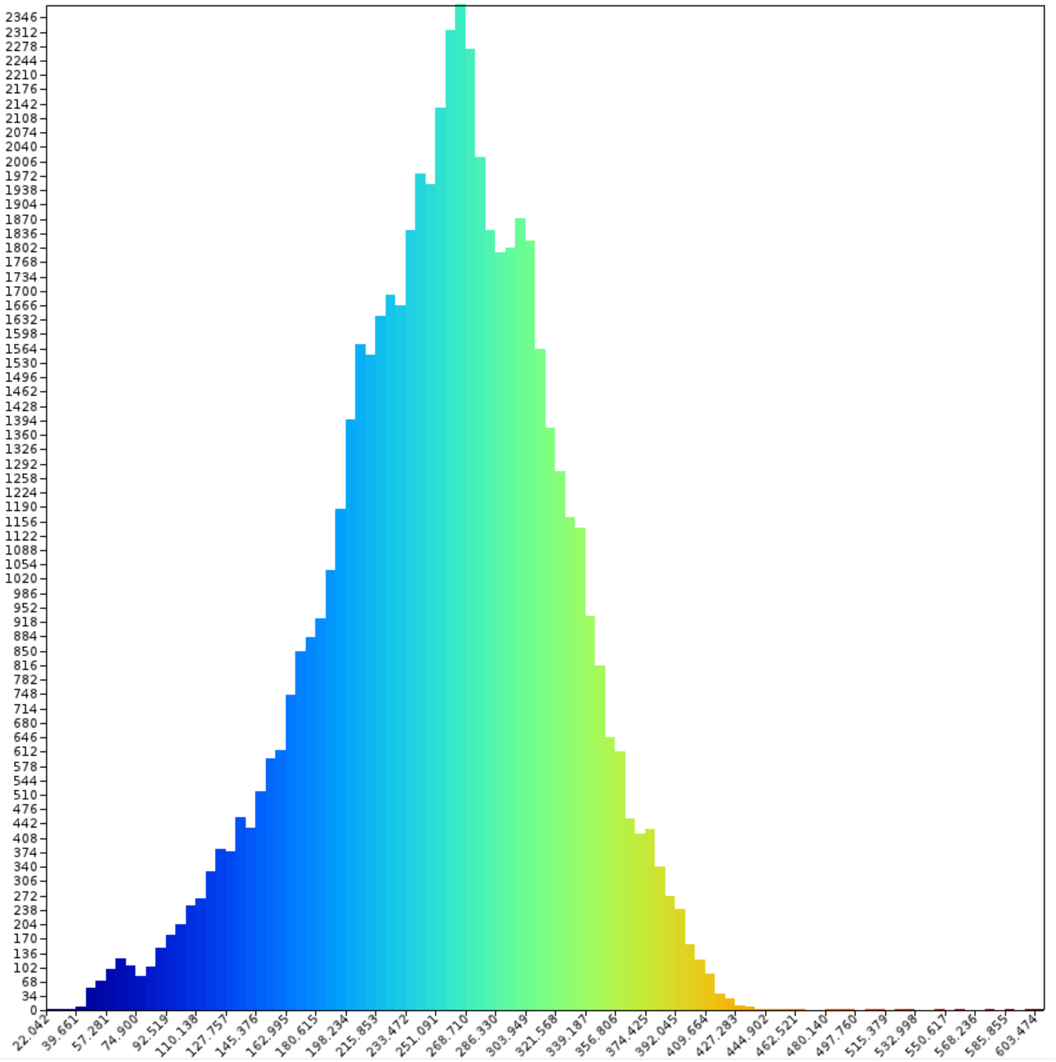

Figure 10. Histogram of wind energy density observed from 164 ENVISAT ASAR wind maps offshore in South India. The x-axis shows wind power density in W/m^2 and the y-axis shows number of grid cells.

4 QuikSCAT winds

The scatterometer QuikSCAT on-board the SeaWinds satellite of the US National Aeronautics and Space Administration (NASA) operated from 1999 to 2009. The 10-year archive of ocean wind maps from Remote Sensing Systems (RSS) http://www.ssmi.com/qscat/qscat_browse.html has been used in the present study. Please read more about the QuikSCAT data in [3]. The data availability is shown in Figure 11 jointly for wind mean wind direction and mean wind speed. The data availability is around twice per day at mid-latitude giving around 7300 samples, one each morning, one each evening for 10 years. However near the Equator the coverage is reduced. Figure 11 shows up to around 4650 samples; this number is excluding rain contaminated observations.

For four locations in the area monthly mean wind speed and wind roses are extracted and shown in Figure 13 and Figure 14, respectively. Figure 15 shows the 10-year averages as a function of month for wind direction and wind speed for the four points.

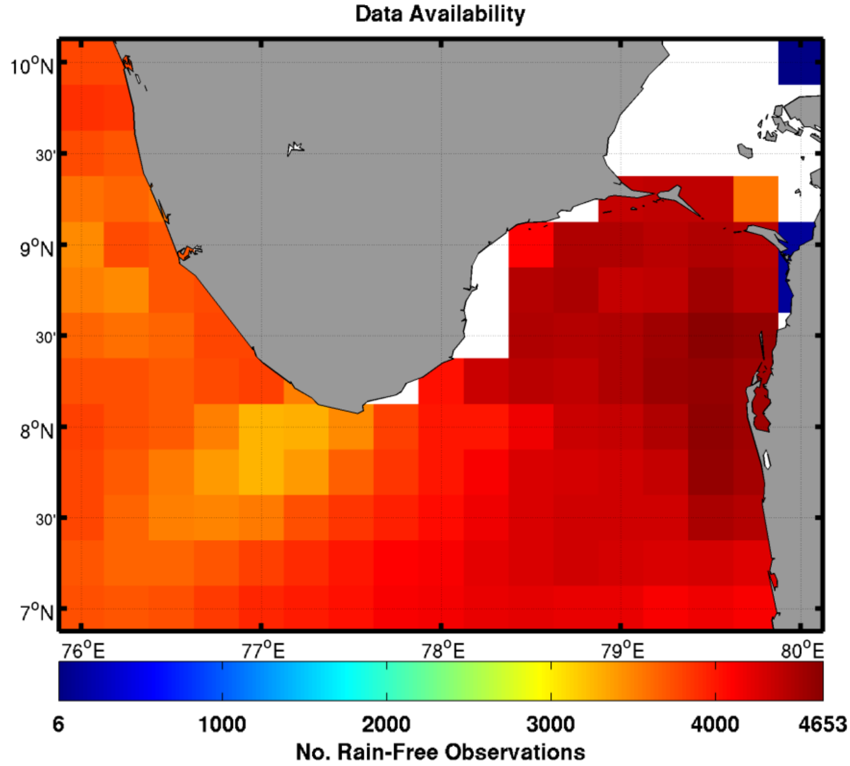
Data Availability
10°N
30'
9°N
30'
8°N
30'
7°N
76°E
77°E
78°E
79°E
80°E
6
1000
2000
3000
4000
4653
No. Rain-Free Observations

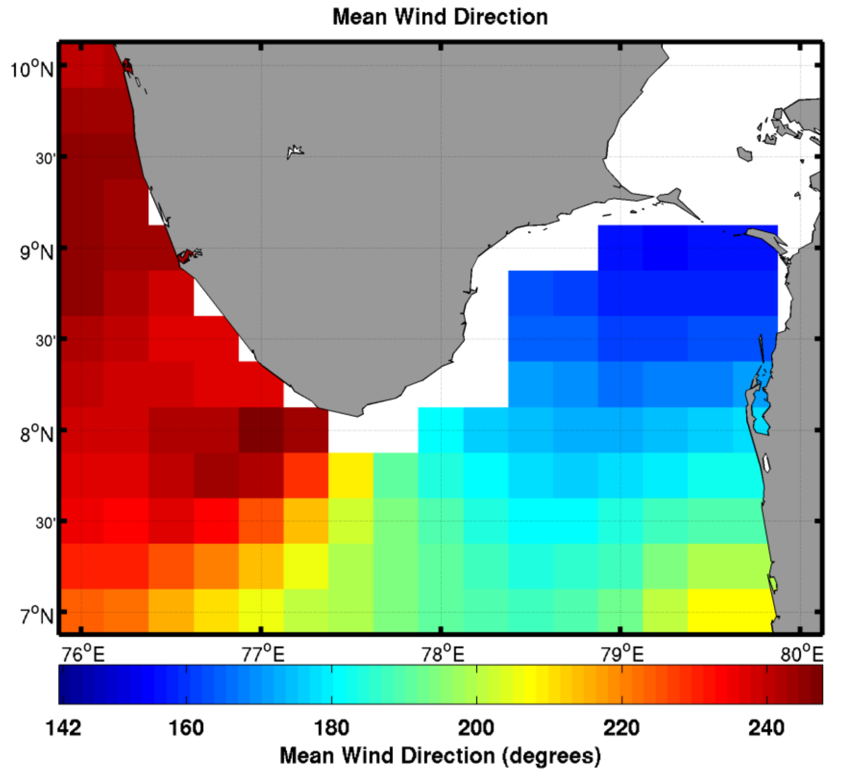
Mean Wind Direction
10°N
30'
9°N
30'
8°N
30'
7°N
76°E
77°E
78°E
79°E
80°E
142
160
180
200
220
240
Mean Wind Direction (degrees)

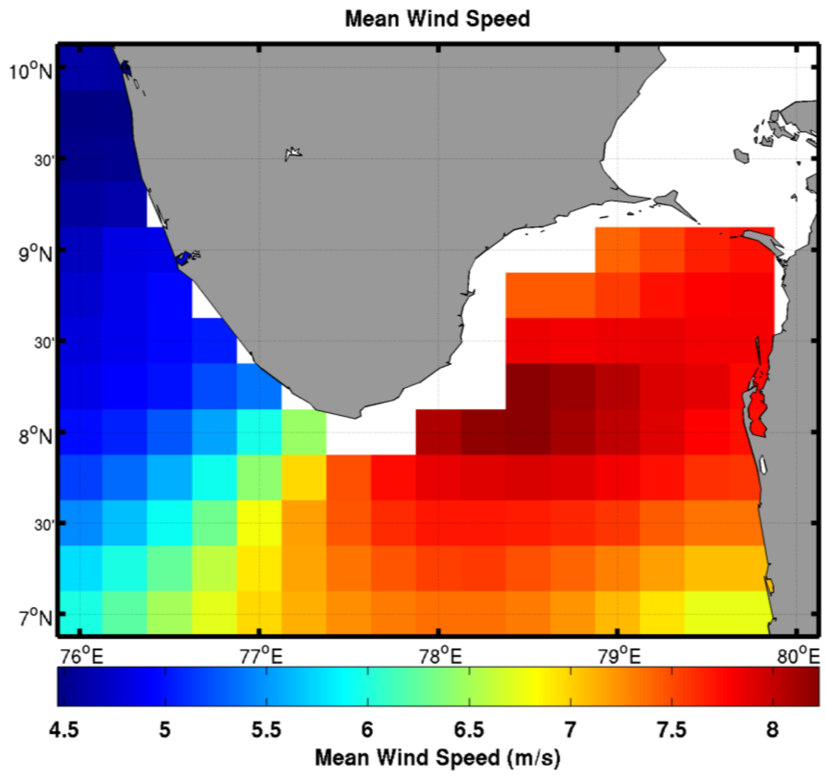

Figure 11. QuikSCAT ocean wind maps showing data availability, mean wind direction and mean wind speed. Data are from RSS.

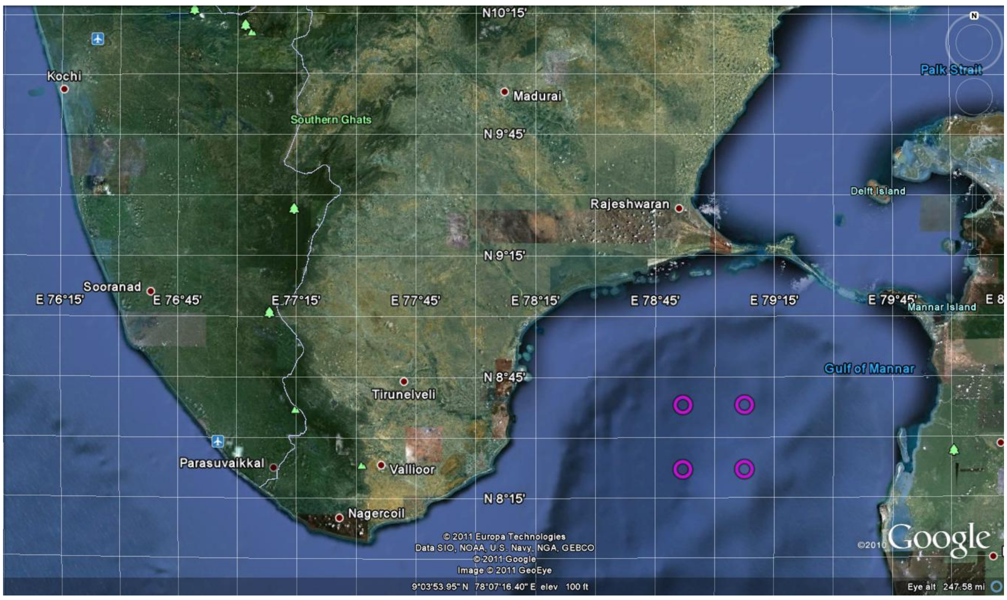

Figure 12. Map showing with pink the four point locations for which QuikSCAT winds have been extracted.

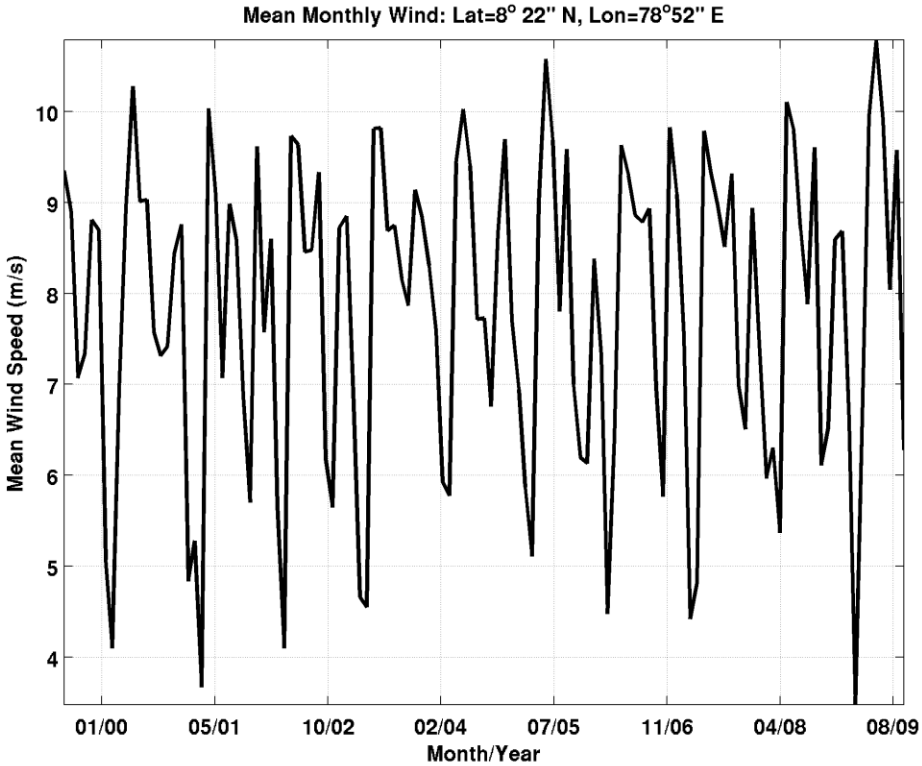
Mean Monthly Wind: Lat=8° 22" N, Lon=78°52" E
Mean Wind Speed (m/s)
10
9
8
7
6
5
4
01/00
05/01
10/02
02/04
07/05
11/06
04/08
08/09
Month/Year

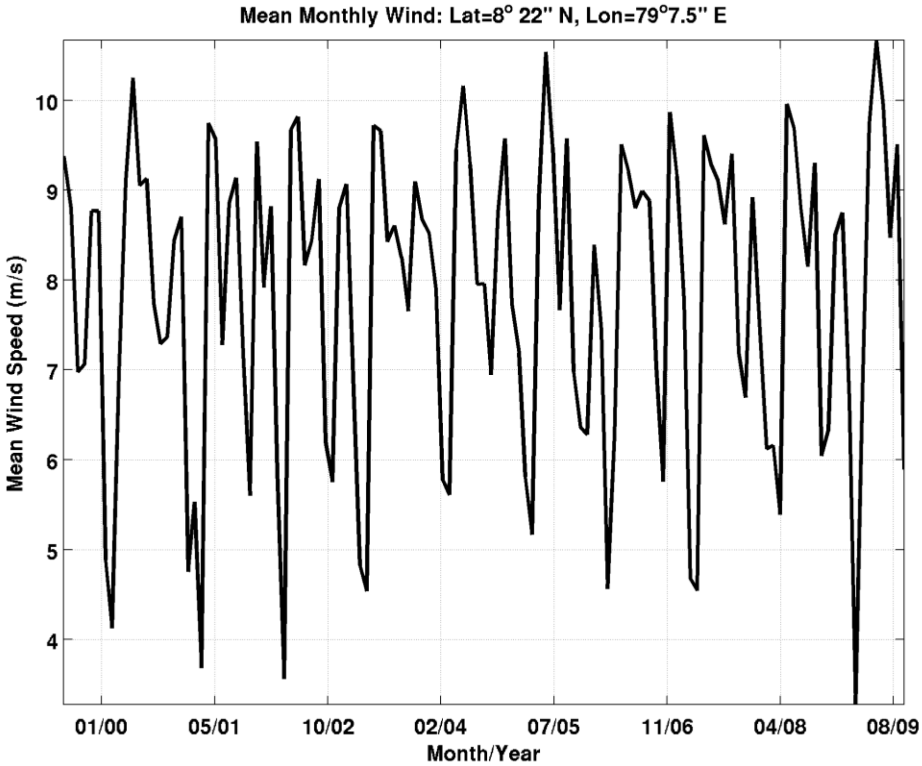
Mean Monthly Wind: Lat=8° 22" N, Lon=79°7.5" E
Mean Wind Speed (m/s)
10
9
8
7
6
5
4
01/00
05/01
10/02
02/04
07/05
11/06
04/08
08/09
Month/Year

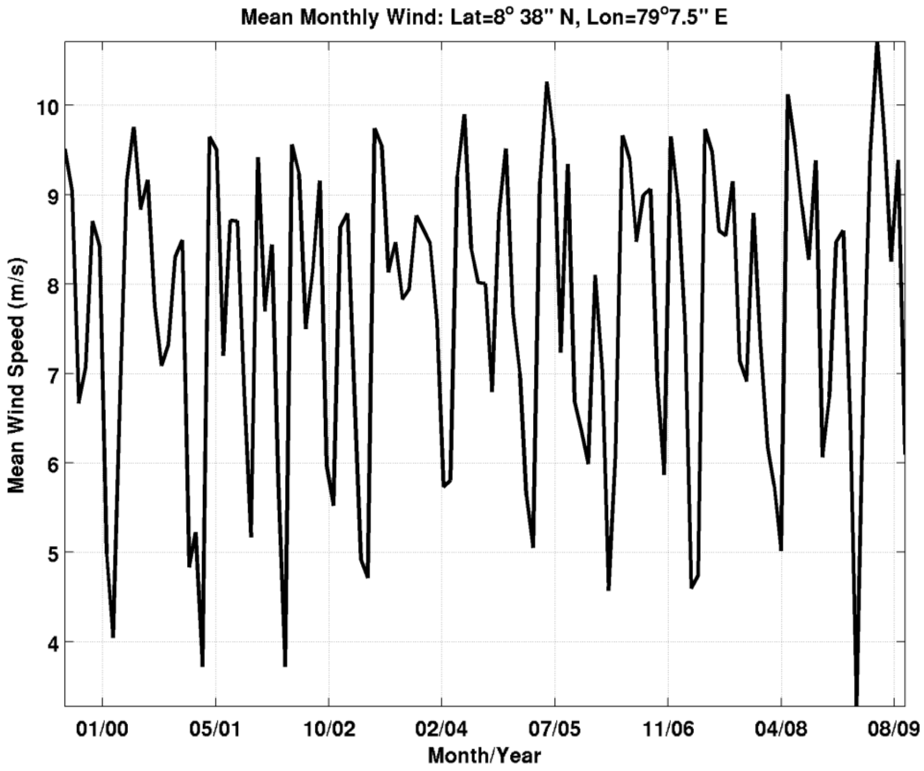

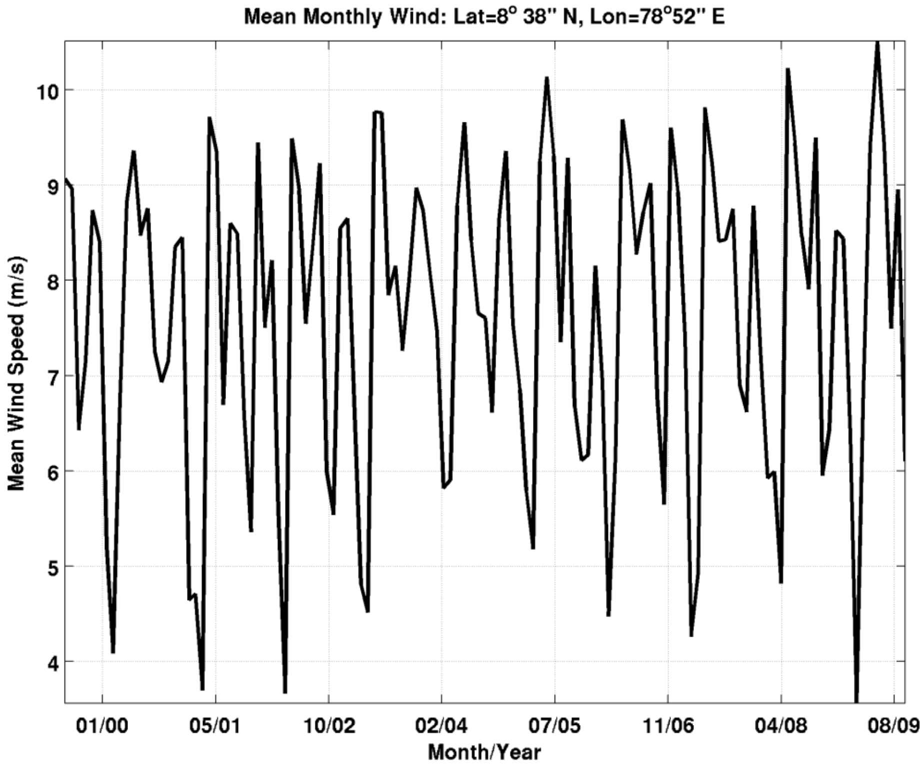

Figure 13. QuikSCAT ocean wind monthly means from10 years for four locations. Data are from RSS. The x-axis shows time month/year.

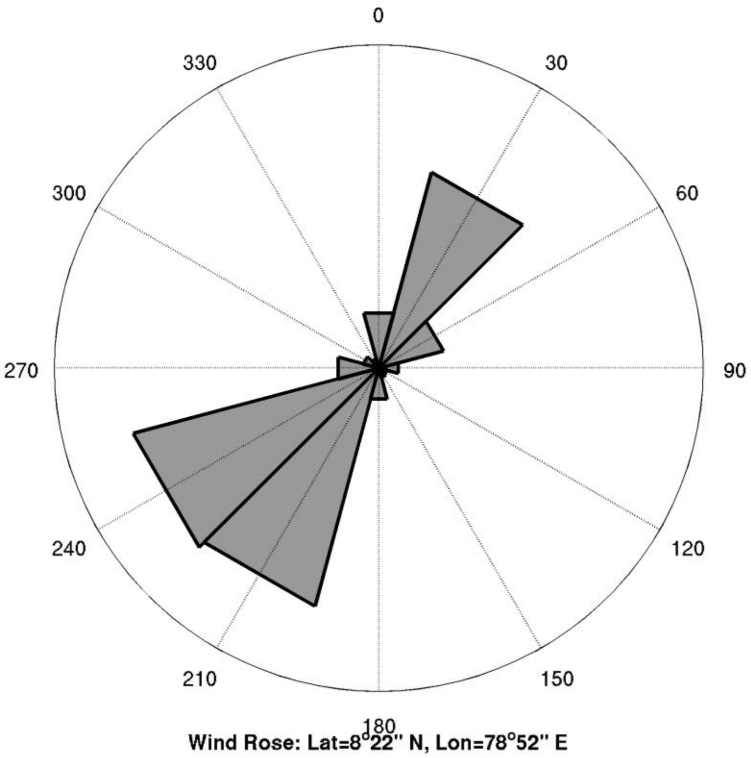

Wind Rose: Lat=8°22'' N, Lon=78°52'' E

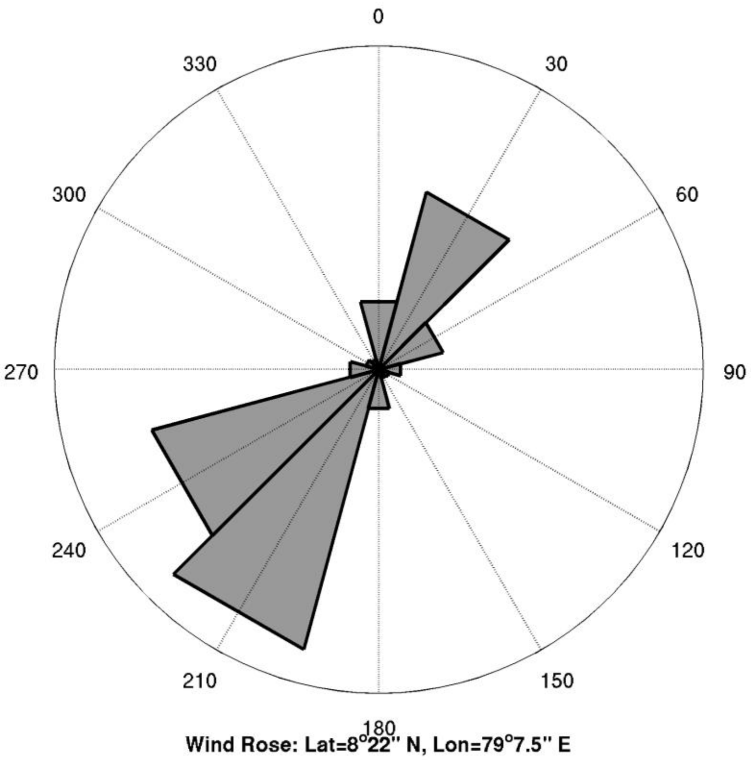

Wind Rose: Lat=8°22'' N, Lon=79°7.5'' E

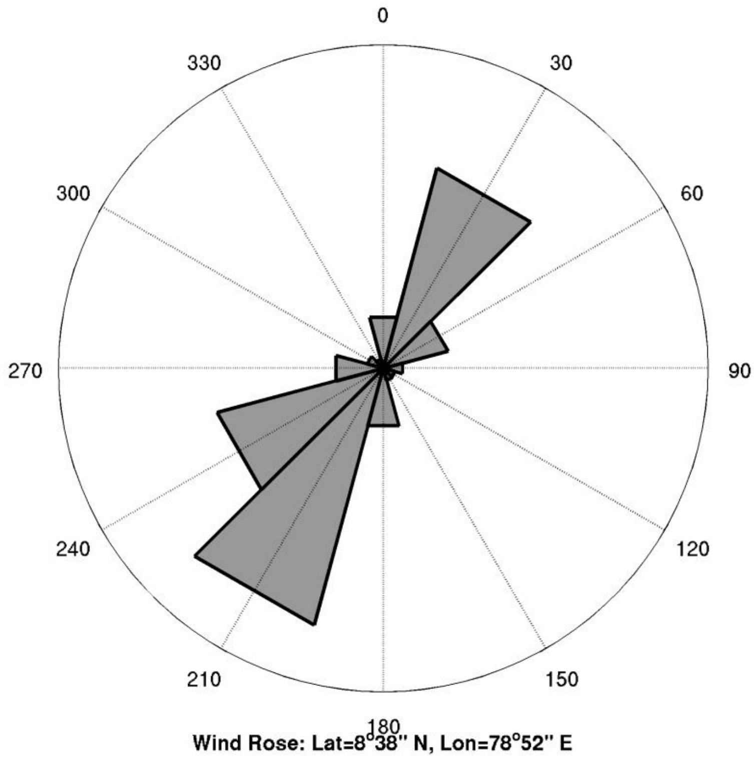

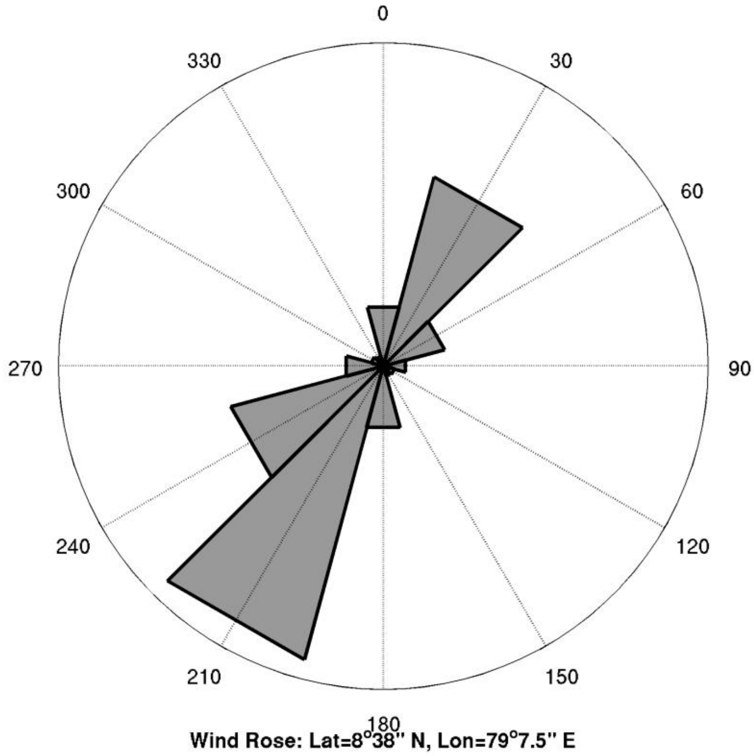

Figure 14. QuikSCAT ocean winds wind roses from10 years for four locations. Data are from RSS.

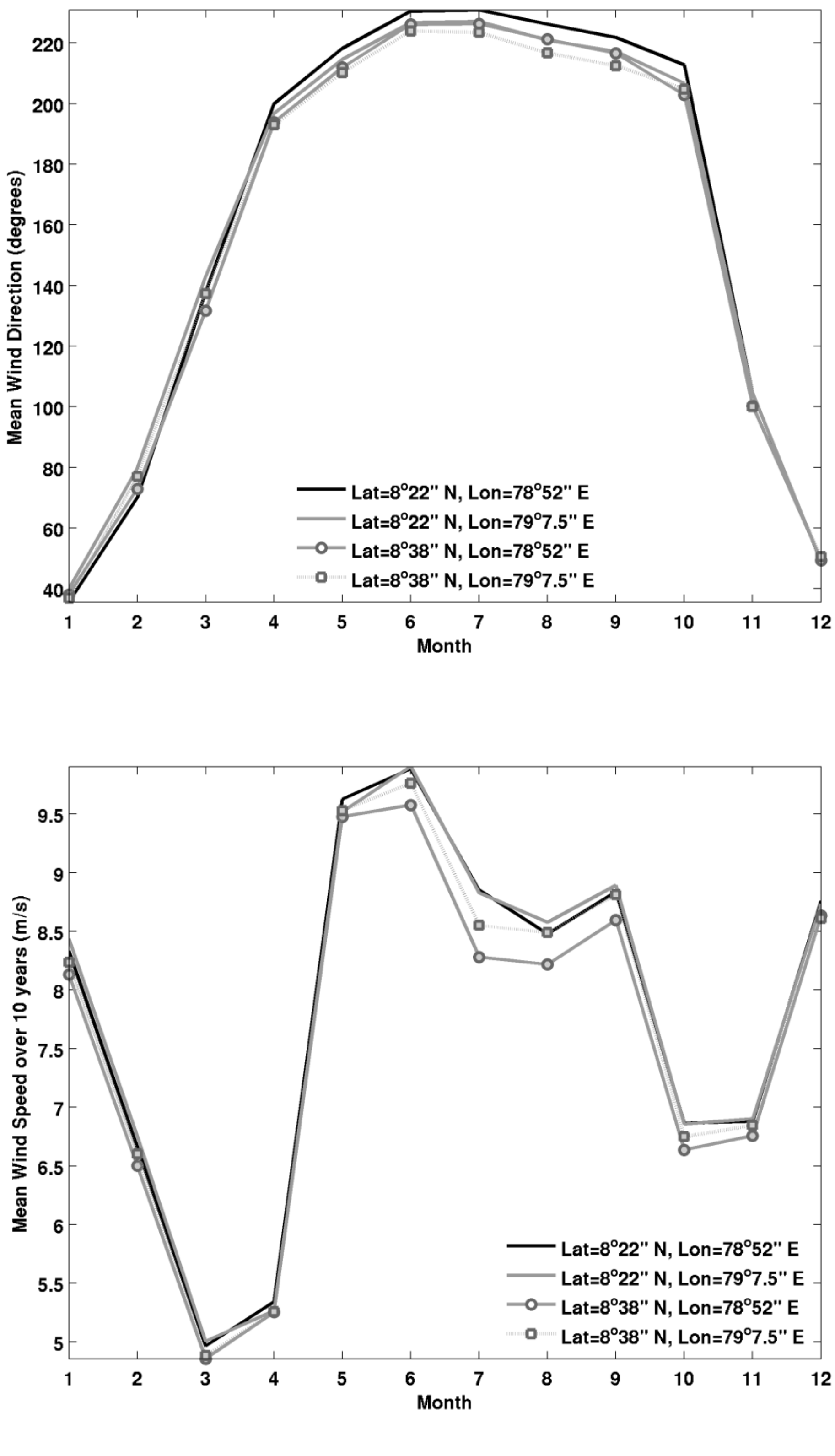

Figure 15. QuikSCAT ocean winds 10-year average per month for the four points, upper shows mean wind direction, lower panel mean wind speed. Data are from RSS.

5 Description of general winds

From a global perspective, the tropical regions of the Earth are characterized by lower wind speeds when compared with the middle and high latitudes. The characteristic feature of the Indian climate is the combination of global circulation (trade winds) and the regional wind systems (monsoons). With the result of these climatic systems, India gets four different seasons. They are winter (Dec-Jan-Feb), pre-monsoon summer (Mar-Apr-May), monsoon (Jun-Jul-Aug) and post-monsoon (Sep-Oct-Nov).

During the summer the entire Asian continent is heated considerably so that the pressure drops down and develops the temperature contrasts between the land mass and surrounding seas. In the beginning of June, the cooler and more humid winds from the Arabian Sea and the Bay of Bengal penetrate over land mass of India. The monsoon from the Arabian Sea is roughly three times stronger than the Bay of Bengal branch. This is the start of southwest monsoon and it intensifies till the end of July and weakens and disappears in the end of August or start of September. The south west monsoon sets in over the extreme south of Indian peninsula (coast of Kerala) generally around the first week of June. The arrival of the monsoon is a gradual process, with a period of transition spread over a week or more. Subsequently, the monsoon from the Arabian Sea advances along the west coast up to Himalaya through Thar Desert and the monsoon from the Bay of Bengal initially tracks the Coromandal coast swerves to the northwest towards the Indo-Gangetic plain. Over seventy percent of India's annual rainfall as well as winds are received during the southwest monsoon.

The temperature gradually falls in the country after September. As the sun moves to the south of the equator, the country experiences cool weather, with temperatures decreasing by about 0.5°C for every 1° towards northern latitude. During October to December, the land mass cools giving rise to a high pressure area with its centre over eastern Siberia. The air begins flowing from the land towards the sea, which is now the area of low pressure, as the northeast monsoon current from the beginning of October. The northeast monsoon lasts through the pre-monsoon seasons, and only ends in March, carries winds that have already lost their moisture while crossing central Asia and the vast rain shadow region lying north of the Himalayas. They cross India diagonally from northeast to southwest. However, south India receives good rainfall during these periods. Some parts of West Bengal, Orissa, Andhra Pradesh, Tamil Nadu, Kerala, Karnataka and North-East India also receive minor precipitation from the northeast monsoon. In most parts of India, this period marks the transition from wet to dry seasonal conditions.

The period from March to May (April to July in North and northwestern India) is generally referred as pre monsoon (summer) season and winds are very poor. However, these climatological features are not steady and smooth flow of air circulation systems. This tropical region sometimes experiences the most violent weather disturbances in the world. Tropical cyclo-genesis is common in the northern reaches of the Indian Ocean in and around the Bay of Bengal. Cyclones bring with them heavy rains, storm surges, and winds that often cut affected areas off from relief and supplies. In the North Indian Ocean Basin, the cyclone season runs from April to December, with peak activity between May and November. During summer, the Bay of Bengal is subjected to intense heating, giving rise to humid and unstable air masses that morph into cyclones.

The 1737 Calcutta cyclone, the 1970 Bhola cyclone, and the 1991 Bangladesh cyclone rank among the most powerful cyclones to strike India, devastating the coasts of eastern India and neighboring Bangladesh. Cyclone 05B, a super cyclone that struck Orissa on 29 October 1999, was the deadliest in more than a quarter-century. With peak winds of 71 m/s, it was the equivalent of a Category 5 hurricane. Widespread death and property destruction are reported every year in the exposed coastal states of West Bengal, Orissa, Andhra Pradesh, and Tamil Nadu. India's western coast, bordering the more placid Arabian Sea, experiences cyclones only rarely; these mainly strike Gujarat and, less frequently, Kerala.

The land and sea breezes are quite common in Indian coasts. It is a relatively shallow system, with a depth of 500-1000m, which penetrates inland up to about 50 km and sometimes as far as 150 km.

6 Discussion

The results from ENVISAT ASAR are of high spatial resolution, 0.01 degree by 0.01 degree, roughly 1 km by 1 km. The accuracy on ocean wind mapping from ENVISAT ASAR is shown to be around 1.3 m/s in the North Sea[4-6] and in the Baltic Sea[7]. The number of SAR wind maps is only 164. This means from a statistical point of view the uncertainty is rather high on the results.

To investigate ocean winds further from satellite also QuikSCAT winds have been studied from the area. These results show strong yearly variation with minimum winds in March and April and relatively low winds in October and November. High winds are found in May to September and in December. The monthly variation from year to year is moderate and the wind roses clearly are dominated by strong winds from the southwest and weaker winds from the northeast. Other wind directions hardly ever occur. Another important feature seen from the QuikSCAT analysis is the much higher winds on the eastern shore compared to the western shore of south India. QuikSCAT has the advantage of a 10-year long time series of ocean wind data with more than 3000 ocean wind maps included in the analysis. The disadvantage is that data does not cover very near-coastal areas. In contrast, the SAR-based results cover very close to the coastline.

Figure 16 is included to make a direct comparison between the two results of mean wind speed. Please note that the number of observations (164 SAR wind maps vs. more than 3000 QuikSCAT wind maps) used and the time (different orbital parameters) are different. Both maps indicate the strongest mean wind speeds around 7.5 m/s in the area from 78° to 79° eastern longitude to 8°0’ to 8°15’ northern latitude.

Using general information on the monsoons in India it appears that the typical winds are also found in the satellite observations comparing the monthly variations in direction and wind speed levels per month for a 10-year period using QuikSCAT satellite images.

It will be necessary to observe winds at higher levels to ascertain the wind profile and thus the energy density at higher levels.

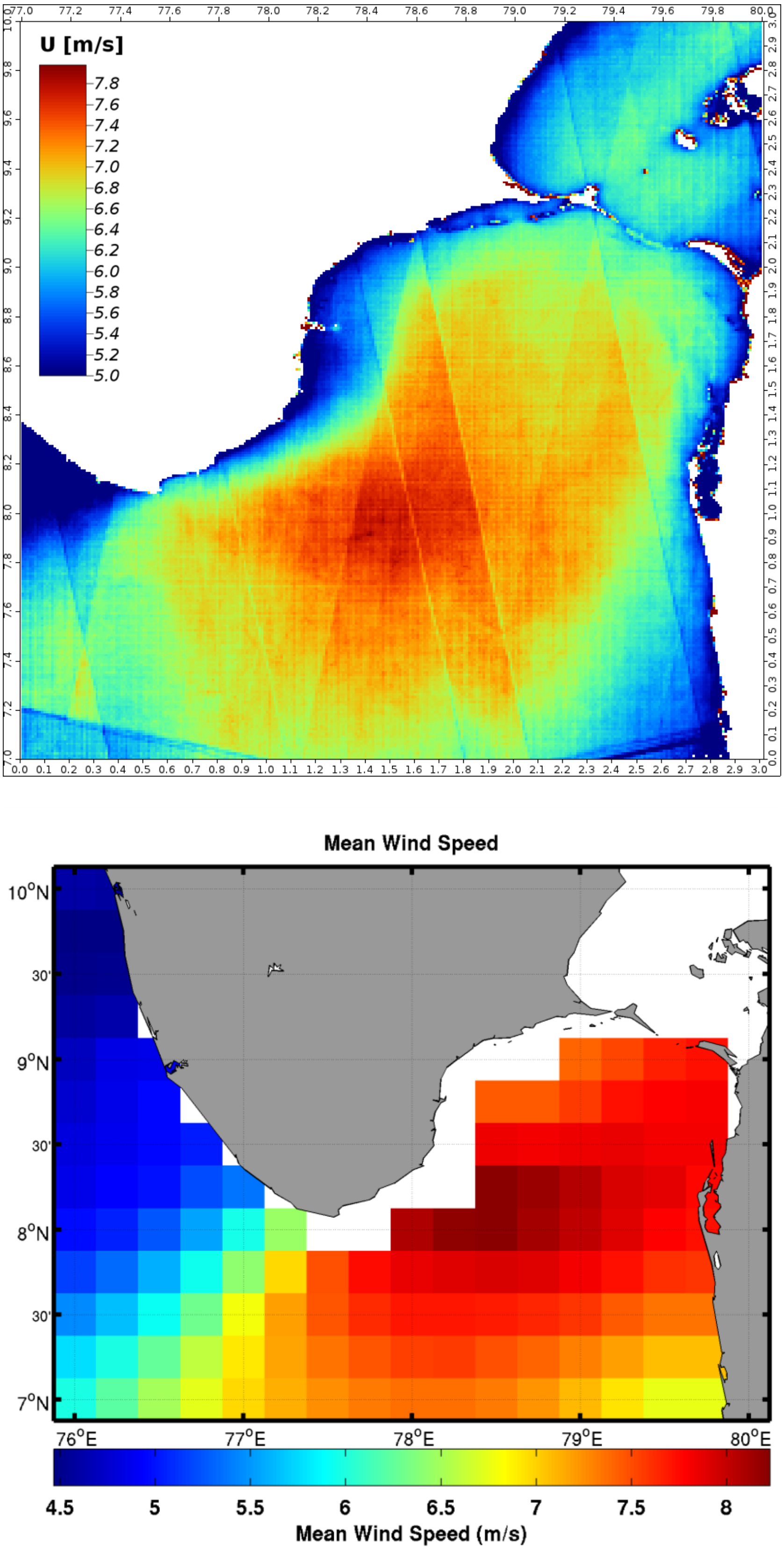

Figure 16. Comparing mean winds from ENVISAT SAR (from ESA) and from QuikSCAT (NASA/ RSS).

Sites with promising winds appear to be located relatively close to the coastline in two areas, see sites 1 and 2 in the north and sites 3 and 4 in the south (Figure 17). Strong winds prevail in the central part far offshore, site 5. In regard to practicalities on grid connection, it is thus concluded that there are two dominant areas of interest for further investigation using ground-based observations in order to understand also the vertical variation of winds prior to wind farm planning offshore. The two promising areas are the northern area (sites 1 and 2) and the southern area (site 3 and 4).

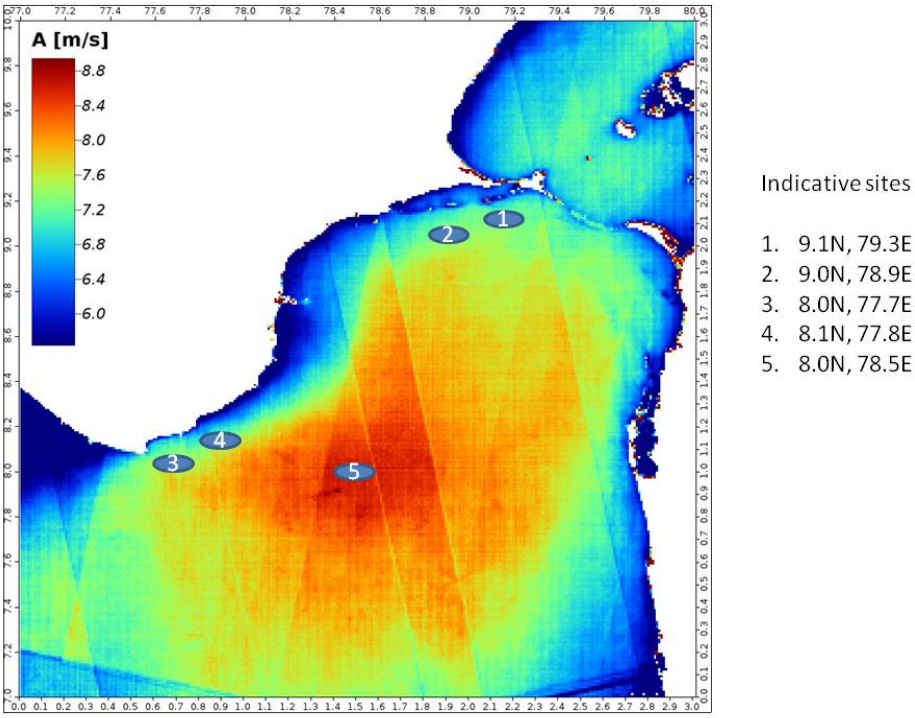

Figure 17. Map showing indicative sites where the mean wind speed, Weibull A, and the wind power density are high.

7 Summary

The offshore wind statistics based on ENVISAT ASAR presented are part of collaboration and research efforts of C-WET and Risø DTU. The aim is to characterize the offshore winds in South India. The major findings are that the winds observed by satellite compare well to general wind circulation temporally. Wind speed and direction during the monsoon and other seasons follow this closely. The strongest winds are from the southwest but also winds from the northeast are relatively high. Winds from other directions are seldom observed.

The mean wind speed near the coast is around 4 to 5 m/s whereas up to 7.6 m/s are found further offshore indicating wind resources from 200 to 500 W/m^2. This is for 10 m above sea level. Five indicative areas of special interest are identified. Two of these are located in the northern part and two in the southern part along the coast. The fifth is far offshore and less likely to be relevant due to logistics (e.g. grid connection). It is recommended to observe winds at several heights to ascertain winds at hub height. The risk of cyclones cannot be assessed from the satellite archive and has to be understood from other sources.

8 Conclusions

ENVISAT ASAR satellite scenes have been retrieved and processed into ocean wind maps by Risø DTU. Further, the wind maps have been analysed in software S-WAsP and the results reported on mean wind speed, Weibull statistics and wind energy density shows pre-feasibility potential for offshore wind energy in South India. Also QuikSCAT satellite wind data have been analyzed and the results compare well both to the SAR-based results as well as to general circulation in India with monsoon. The recommendation is to focus on the indicative areas in the north along the coast and in the south. It is important to observe winds up to hub height. In the future mast observations could be compared to the satellite-based results.

References

1. Christiansen, M. B.; Hasager, C. B.; Thompson, D. R.; Monaldo, F. Ocean winds from synthetic aperture radar. In *Ocean remote Sensing: Recent Techniques and Applications.*, Niclos, R., Caselles, V., Eds.; Research Singpost Editorial: **2008**; pp 31-54.

2. Pryor, S. C.; Nielsen, M.; Barthelmie, R. J.; Mann, J. Can satellite sampling of offshore wind speeds realistically represent wind speed distributions? Part II Quantifying uncertainties associated with sampling strategy and distribution fitting methods. *Journal of Applied Meteorology* **2004**, *43*, 739-750.

3. Peña, A.; Hahmann, A.; Hasager, C. B.; Bingöl, F.; Karagali, I.; Badger, J.; Badger, M.; Clausen, N. E. *South Baltic Wind Atlas*; Risø-R-1775; Roskilde, **2011**.

4. Badger, M.; Badger, J.; Nielsen, M.; Hasager, C. B.; Peña, A. Wind class sampling of satellite SAR imagery for offshore wind resource mapping. *Journal of Applied Meteorology* **2010,** *49* (12), 2474-2491.

5. Christiansen, M. B.; Koch, W.; Horstmann, J.; Hasager, C. B. Wind resource assessment from C-band SAR. *Remote Sensing of Environment* **2006,** *105*, 68-81.

6. Hasager, C. B.; Barthelmie, R. J.; Christiansen, M. B.; Nielsen, M.; Pryor, S. C. Quantifying offshore wind resources from satellite wind maps: study area the North Sea. *Wind Energy* **2006,** *9*, 63-74.

7. Hasager, C. B.; Badger, M.; Peña, A.; Larsén, X. G.; Bingöl, F. SAR-Based Wind Resource Statistics in the Baltic Sea. *Remote Sensing* **2011,** *3* (1), 117-144.

Appendix 1

List of the ENVISAT ASAR scenes used for the analysis. The list shows for each scene the Polarization (Pol), which is either horizontal transmit and receive (h) or vertical transmit and receive (v), Date and Time (UTC).

Pol	Date	Time
	(yyyymmdd)	(hhmmss)
v	20021123	170212
v	20021126	042905
v	20021206	165339
v	20021221	044310
v	20021222	165047
v	20021225	165628
v	20030103	043443
v	20030107	164758
v	20030119	043153
v	20030204	042903
v	20030214	165336
v	20030302	165046
v	20030305	165628
v	20030314	043444
v	20030415	042907
v	20030504	043156
v	20030624	042908
v	20030704	165344
h	20030713	043159
v	20030720	165057
v	20030723	165638
h	20030801	043453
v	20030817	043203
v	20030817	043217
v	20030912	165351
v	20030928	165057
v	20031001	165638
v	20031007	042912
h	20031010	043450
v	20031014	164807
v	20031026	043200
v	20031111	042909
v	20031121	165345
h	20031130	043202
v	20031207	165057
v	20031210	165637

Pol	Date	Time
	(yyyymmdd)	(hhmmss)
v	20031223	164808
v	20040104	043203
v	20040107	043742
v	20040114	165636
v	20040117	170215
v	20040130	165344
v	20040202	165925
v	20040215	165054
v	20040227	043448
v	20040302	164805
v	20040314	043202
v	20040327	170218
v	20040330	042911
h	20040402	043449
v	20040409	165344
v	20040424	044319
v	20040425	165055
v	20040507	043448
v	20040510	044029
v	20040511	164805
v	20040523	043203
v	20040526	043743
v	20040602	165640
v	20040605	170221
v	20040608	042915
v	20040811	165652
v	20040912	165057
v	20040924	043448
v	20040928	164806
v	20041010	043203
v	20041020	165641
v	20041026	042915
v	20041108	165928
v	20041117	043741
v	20041203	043457
v	20041206	044031

Pol	Date	Time
	(yyyymmdd)	(hhmmss)
V	20041207	164806
V	20041229	165603
V	20050309	165635
V	20050312	170215
V	20050325	165344
V	20050328	165925
V	20050409	044322
V	20050425	044035
V	20050426	164811
V	20050518	165642
V	20050521	170222
V	20050603	165350
V	20050618	044326
V	20050619	165102
V	20050730	170221
V	20050815	165922
V	20051005	165638
V	20051008	170218
V	20051021	165349
V	20051024	165929
V	20051105	044323
V	20051121	044031
V	20051217	170212
V	20051227	164759
v	20060114	044309
v	20060130	044021
v	20060225	170208
v	20060307	164757
v	20060313	165917
v	20060325	044309
v	20060603	044316
v	20060604	165044
v	20060712	165639
v	20060715	170219
v	20060813	165057
v	20060923	170214
h	20061003	164805
v	20061006	165345
v	20061009	165926
v	20061110	165319
v	20061119	043200
v	20061202	170206

Pol	Date	Time
	(yyyymmdd)	(hhmmss)
v	20061218	165915
v	20061230	044258
v	20061231	165053
v	20070220	164801
v	20070226	165922
v	20070418	165631
v	20070421	170212
v	20070507	165914
v	20070520	165044
v	20070826	043158
v	20070908	170202
v	20070921	165339
v	20080204	044008
v	20080307	043442
v	20080504	165047
v	20080507	165628
v	20080510	170208
v	20080520	164758
v	20080523	165338
v	20080526	165918
v	20080729	164759
h	20081111	164738
v	20081203	165625
v	20081206	170156
v	20081216	164749
v	20090211	165626
v	20090214	170206
v	20090227	165336
v	20090302	165916
v	20090422	165625
v	20090425	170205
v	20090505	164755
v	20090508	165335
v	20090511	165916
v	20090814	043440
v	20090905	044308
v	20090912	170204
v	20091108	043133
v	20091121	170201
v	20091127	043433
v	20091226	170200
v	20100215	165908

v	20100328	043144		h	20101204	043006
v	20100331	043724		h	20110320	044349
v	20100508	044302		h	20110403	043232
v	20100925	044300		h	20110422	043408

Appendix 2

Description of data files delivered with this report.

SAR winds

The wind resource maps from satellite SAR are delivered in two formats:

1. Multi-layer *.cdf* files containing all parameters (e.g. N, U, Weibull A and k, E, and geographical coordinates) calculated from three different fitting methodologies (2nd moment, 3rd moment, and WAsP):

```
India.2ndMoment.cdf
India.3rdMoment.cdf
India.WAsP.cdf
```

2. GIS-compatible *.grd files* containing single parameters for each of the three different fitting methodologies applied (2nd moment, 3rd moment, and WAsP):

```
India.M2.A.bin.grd
India.M2.E.bin.grd
India.M2.MP.bin.grd
India.M2.k.bin.grd

India.M3.A.bin.grd
India.M3.E.bin.grd
India.M3.MP.bin.grd
India.M3.k.bin.grd

India.WAsP.A.bin.grd
India.WAsP.E.bin.grd
India.WAsP.MP.bin.grd
India.WAsP.k.bin.grd

India.F.bin.grd
India.N.bin.grd
India.WD.bin.grd
India.WS.bin.grd
India.WSs.bin.grd
```

Uncertainty of SAR winds

Sampling uncertainties related to the SAR based wind resource maps are provided as separate files. Uncertainties are given in two different file formats for the 2nd and 3rd moment method (uncertainties for the 3rd moment and the WAsP method are identical, therefore the latter is not provided):

1. ASCII text files:

Uncertainty_of_U.xyz: Uncertainty of WS and StdDev of it. Fields are X[o], Y[o], WS[m/s], WSs[m/s^2].

Uncertainty_of_M2.xyz: Uncertainty of calculated A, k parameters and derived power density value with 2nd moment. Fields are X [o], Y[o], E[W/m^2], A[m/s], k[-], and an extra field for the Covariance of A and k.

```
Uncertainty_of_M3.xyz: Uncertainty of calculated A, k
parameters and derived power density value with 3rd moment.
Fields are X [o], Y[o], E[W/m^2], A[m/s], k[-], and an
extra field for the Covariance of A and k.
```

2. GIS-compatible *.grd files* containing all the variables listed under 1) in alatitude-longitude coordinate system:

```
Uncertainty_M2_A.grd
Uncertainty_M2_CovAk.grd
Uncertainty_M2_E.grd
Uncertainty_M2_k.grd
Uncertainty_M3_A.grd
Uncertainty_M3_CovAk.grd
Uncertainty_M3_E.grd
Uncertainty_M3_k.grd
Uncertainty_WS.grd
Uncertainty_WSs.grd
```

QuikSCAT winds

Wind speed and direction have been extracted from the QuikSCAT data set for the grid cells closest to the five indicative sites (see Figure 17). Note that the QuikSCAT data presented in this report cover four different point locations (see Figure 11-16). The QuikSCAT wind data are provided in *.csv* format:

```
p1_8.00N_77.12E.csv
p2_8.02N_77.13E.csv
p3_8.00N_78.08E.csv
p4_9.00N_78.88E.csv
p5_9.02N_79.05E.csv
```

The QuikSCAT winds are also provided as a single WAsP *.wcp* file:

```
SI.wcp
```

Risø DTU is the National Laboratory for Sustainable Energy. Our research focuses on development of energy technologies and systems with minimal effect on climate, and contributes to innovation, education and policy. Risø has large experimental facilities and interdisciplinary research environments, and includes the national centre for nuclear technologies.

Risø DTU
National Laboratory for Sustainable Energy
Technical University of Denmark

Frederiksborgvej 399
PO Box 49
DK-4000 Roskilde
Denmark
Phone +45 4677 4677
Fax +45 4677 5688

www.risoe.dtu.dk